Accepted Manuscript

Biotrickling filter modeling for styrene abatement. Part 2: Simulating a two-phase partitioning bioreactor

Pau San-Valero, Antonio D. Dorado, Guillermo Quijano, F. Javier Álvarez-Hornos, Carmen Gabaldón

Chemosphere

Please cite this article as: Pau San-Valero, Antonio D. Dorado, Guillermo Quijano, F. Javier Álvarez-Hornos, Carmen Gabaldón, Biotrickling filter modeling for styrene abatement. Part 2: Simulating a two-phase partitioning bioreactor, *Chemosphere* (2017), doi: 10.1016/j.chemosphere. 2017.10.141

Highlights

A dynamic model was applied to simulate two-phase biotrickling filters

The model was calibrated with several inlet loadings conditions

Validation was performed with the data from dynamic loading fluctuations

Superior performance versus biotrickling filters relied on greater mass transfer

Use of two-phase biotrickling was recommended for mass transfer limited systems

Biotrickling filter modeling for styrene abatement. Part 2:

Simulating a two-phase partitioning bioreactor

Pau San-Valero[a], Antonio D. Dorado[b], Guillermo Quijano[c], F. Javier Álvarez-Hornos[a],

Carmen Gabaldón[a*]

[a] Research Group GI²AM, Department of Chemical Engineering, Universitat de Valencia,

Av. de la Universitat s/n, 46100 Burjassot, Spain. Tel. +34 963543437, Fax: +34 3544898

[b] Department of Mining Engineering and Natural Resources, Universitat Politècnica de

Catalunya, Bases de Manresa 61-73,08240, Manresa, Spain

[c] CONACYT – Laboratory for Research on Advanced Processes for Wastewater Treatment,

Engineering Institute, Juriquilla Academic Unit, National Autonomous University of México

(UNAM), Blvd. Juriquilla 3001, Querétaro 76230, Mexico

[*] Corresponding author: carmen.gabaldon@uv.es

19 **Abstract**

20 A dynamic model describing styrene abatement was developed for a two-phase partitioning

21 bioreactor operated as a biotrickling filter (TPPB-BTF). The model was built as a coupled set

22 of two different systems of partial differential equations depending on whether an irrigation

23 or a non-irrigation period was simulated. The maximum growth rate was previously

24 calibrated from a conventional BTF treating styrene (Part 1). The model was extended to

25 simulate the TPPB-BTF based on the hypothesis that the main change associated with the

26 non-aqueous phase is the modification of the pollutant properties in the liquid phase. The

27 three phases considered were gas, a water–silicone liquid mixture, and biofilm. The selected

28 calibration parameters were related to the physical properties of styrene: Henry's law

29 constant, diffusivity, and the gas–liquid mass transfer coefficient. A sensitivity analysis

30 revealed that Henry's law constant was the most sensitive parameter. The model was

31 successfully calibrated with a goodness of fit of 0.94. It satisfactorily simulated the

32 performance of the TPPB-BTF at styrene loads ranging from 13 to 77 g C m^{-3} h^{-1} and empty

33 bed residence times of 30–15 s with the mass transfer enhanced by a factor of 1.6. The model

34 was validated with data obtained in a TPPB-BTF removing styrene continuously. The

35 experimental outlet emissions associated to oscillating inlet concentrations were satisfactorily

36 predicted by using the calibrated parameters. Model simulations demonstrated the potential

37 improvement of the mass-transfer performance of a conventional BTF degrading styrene by

38 adding silicone oil.

39

40 **Keywords:** Biological air treatment; Biotrickling filter; Mathematical modeling; Silicone oil;

41 Styrene; Two-phase partitioning bioreactor

42

2

1. Introduction

One of the main limitations of the abatement of styrene-laden air streams by biotechnological

processes is the poor aqueous solubility of the compound and its toxicity to microbial

communities (Dumont et al., 2014). Therefore, two-phase partitioning bioreactors (TPPBs),

which are biological systems provided with a non-aqueous phase (NAP) with a high affinity

for target pollutants, have been reported as a feasible treatment technology for compounds

such as styrene (Muñoz et al., 2012; Rene et al., 2011; San-Valero et al., 2017). The styrene-

removal enhancement in TPPBs is attributed to the high solubility of styrene in silicone oil,

which is approximately 236 times higher than that in water (Patel et al., 2017). The NAP

addition can also buffer volatile organic compound (VOC)-loading surges and avoid

starvation periods by acting as a pollutant reservoir (Bailón et al., 2009). Several studies have

demonstrated that most NAPs also show a high affinity toward oxygen; consequently, the

oxygen mass transfer rate might also be improved in TPPBs (Daugulis et al., 2011;

Kraakman et al., 2011; Quijano et al., 2009b).

Several experimental studies on VOC removal in TPPBs have focused on the quantification

of mass transport coefficients (Dumont and Andrès, 2012; Hernández et al., 2011;

Moradkhani et al., 2017) and on the process microbiology (Darracq et al., 2012; Karimi et al.,

2013; Ordaz et al., 2014). However, these aspects have not been incorporated in a

comprehensive mathematical description of TPPBs operated as biotrickling filters (TPPB-

BTFs).

TPPB-BTFs present the same reactor configuration as that found in conventional BTFs;

however, the recirculated aqueous solution is provided with the NAP. Although studies on

TPPB-BTFs treating styrene are scarce in the literature (Zamir et al., 2015), compounds with

a similar solubility (e.g., VOCs with dimensionless Henry's law constants between 0.1 and

1.0 at 25°C and 1atm), such as dichloromethane or α-pinene, have been abated satisfactorily

68   in TPPB-BTFs using silicone oil as the NAP (Bailón et al., 2009; Muñoz et al., 2008). In a

69   previous study in our laboratory, we demonstrated that that a TPPB-BTF using industrial-

70   grade silicone oil removed styrene with higher efficiency and stability than a conventional

71   BTF operated under the same conditions (San-Valero et al., 2017). In this study, the removal

72   efficiency (RE) obtained was approximately 40% higher than that of the conventional BTF

73   without an NAP, while supporting a critical inlet load (IL) two times higher than in the

74   conventional BTF.

75   Studies on TPPB-BTF modeling are limited. Parnian et al. (2016) proposed an approach for

76   styrene mass transfer estimation in a BTF with silicone oil from a modeling framework based

77   on general mass balances and transfer equations described by Hernández et al. (2011).

78   Dorado et al. (2015) proposed a novel mathematical description of TPPBs from experimental

79   findings reported in stirred tanks. A comprehensive description of the complex mass transfer

80   phenomena occurring simultaneously in TPPBs was conducted using the partial mass transfer

81   coefficients for both VOCs and oxygen in stirred tanks.

82   TPPB-BTFs are complex multiphase systems that represent a challenge from a mathematical

83   modeling point of view. The occurrence of simultaneous transfer pathways for both VOCs

84   and oxygen makes the experimental determination of individual mass transfer coefficients

85   difficult (Muñoz et al., 2012). On the other hand, most BTF models available in the literature

86   do not consider intermittent irrigation, which is a common practice in industrial BTFs

87   (Sempere et al., 2012). Intermittent irrigation strongly affects the BTF performance;

88   therefore, it must be considered in the mathematical description (San-Valero et al., 2015).

89   Unfortunately, no systematical studies on styrene removal in TPPB-BTFs considering such

90   industrial operating conditions are available in the literature.

91   In this work, a dynamic model for simulating the performance of a TPPB-BTF was assessed

92   by adapting the model developed for a styrene-degrading BTF without a NAP addition,

93   which was presented Part 1. The calibration and validation of the model were conducted

94   using the experimental data from a TPPB-BTF treating styrene using silicone oil as the NAP.

95   The results obtained from the multiphase system were compared with those obtained in a

96   conventional BTF to quantify the potential benefits of adding silicone oil. The

97   phenomenological mathematical model developed in this study aimed to provide a better

98   understanding of the fundamental mechanisms that occur in this bioprocess, so that the

99   critical design and operational parameters could be identified.

100

101   **2. Materials and methods**

102   2.1. Lab-scale plant operation for the TPPB

103   A lab-scale BTF identical to that in Part 1 was used (0.144 m inner diameter, 1.63 m height,

104   working volume of 20 L, working height = 1.23 m) with an external recirculation tank of 6 L.

105   The BTF was packed with polypropylene rings (25 mm nominal diameter, a =207 m^2 m^{-3}, θ_P

106   = 92%). The liquid phase was intermittently irrigated (15 min every 2 h) with a liquid flow of

107   2.7 L min^{-1}. On day 0, 1 L of industrial-grade silicone oil (XIAMETER PMX-200, Univar,

108   Spain) containing culture sludge acclimated to styrene was added to the recirculation tank.

109   The silicone oil percentage was 5% v/v relative to the BTF packed volume. The kinematic

110   viscosity and the density of the silicone oil were 50 cSt and 0.96 g mL^{-1}, respectively. The

111   selected conditions for calibration purposes that corresponded to the average data

112   representing the stable conditions of the TPPB-BTF performance are presented in Table 1.

113   The inlet load (IL) was increased from 22 g C m^{-3} h^{-1} up to 43 g C m^{-3} h^{-1} by decreasing the

114   empty bed residence time (EBRT) from 30 to 15 s. Subsequently, the EBRT was maintained

115   at 15 s and the inlet concentration was increased, resulting in ILs from 13 g C m^{-3} h^{-1} to 77 g

116   C m^{-3} h^{-1}. The resilience of the TPPB-BTF was evaluated by the application of styrene shock

117   loadings under transient conditions with inlet concentrations varying from 100–700 mg C m^{-}

5

118   [3]. The purge of water (3 L) was carried out once per week, and it represented less than 4% of

119   the carbon fed to the reactor during the week. Further details can be found in San-Valero et

120   al. (2017).

121

122   Table 1. Experimental elimination capacity (EC) data (± standard deviation) used for the

123   calibration of the TPPB-BTF model (San-Valero et al., 2017)

Days	IL ($g\ C\ m^{-3}\ h^{-1}$)	Inlet conc. ($mg\ C\ m^{-3}$)	EBRT (s)	EC ($g\ C\ m^{-3}\ h^{-1}$)
20-36	22	184	30	19.0 ± 1.0
38-47	33	184	20	27.1 ± 1.7
50-60	43	181	15	30.8 ± 2.6
62-67	23	98	15	19.1 ± 1.1
68-70	77	323	15	43.2 ± 1.5
71-75	13	55	15	11.7 ± 0.0

124

125   2.2. Model assumptions in the TPPB

126   The dynamic model describing the styrene abatement was extended for a TPPB-BTF based

127   on the previous application of the model to simulate a conventional BTF treating styrene (see

128   Part 1). The model accounted for simulating discontinuous irrigation. At periods without

129   irrigation, the liquid phase was assumed to be a stagnant phase, and the convective transport

130   was excluded in the modeling. One of the most accepted assumptions of TPPB in continuous

131   stirred tank reactors' (CSTR) and aerated tanks' configuration is that the mass transfer

132   between water and a NAP is faster than that between gas and liquid phases; therefore, a

133   water–NAP equilibrium is considered (Dumont and Andrès, 2012; Quijano et al., 2010). This

134   assumption has also been used to represent the gas–liquid mass transfer phenomena in TPPB-

135   BTFs (Hernández et al., 2011; Parnian et al., 2016) and in TPPB-bioscrubbers (Yeom et al.,

136   2010). To extend the model, it was assumed that the hydrodynamics of the BTF are of good

137   mixing, allowing the liquid phase to be considered a pseudo-homogenous mixture of water

138   and silicone. The other key assumptions are based on the previous work of Dorado et al.

6

139   (2015) on the modeling of TPPB-CSTR: (1) the microbial kinetic parameters were assumed

140   to remain the same as the conventional BTF treating styrene ($\mu_{max} = 2.65 \times 10^{-6}\,\text{s}^{-1}$, $Y_{sty} =$

141   0.33, $Y_o = 0.12$, $K_{sty} = 0.154\,\text{g m}^{-3}$, $K_o = 0.26\,\text{g m}^{-3}$, Part 1); (2) based on the fact that silicone

142   oil is approximately 50 times more affine for styrene than for oxygen, it was considered that

143   the effect of the NAP on the oxygen mass transfer was negligible compared with that on the

144   styrene mass transfer. Thus, the same parameters as for oxygen in Part 1 were used ($H_o =$

145   31.4, $D_o = 2.0 \times 10^{-9}\,\text{m}^2\,\text{s}^{-1}$, $K_L a_o = 0.013\,\text{s}^{-1}$, Part 1). Accordingly, the model was based on

146   the hypothesis that the main change in the system performance associated with the addition

147   of a NAP is the modification of the properties of the pollutant in the mixed water–silicone

148   phase. According to these assumptions, the model equations for styrene were modified as

149   follows:

150   Mass balance in the gas phase

151
$$\theta_G \frac{\partial C_{G_{sty}}}{\partial t} = -v_G \frac{\partial C_{G_{sty}}}{\partial z} - K_L a_{mix}\left(\frac{C_{G_{sty}}}{H_{mix}} - C_{L_{sty}}\right) \qquad (1)$$

152   Mass balance in the water–silicone liquid mixture

153
$$\theta_L \frac{\partial C_{L_{sty}}}{\partial t} = v_L \frac{\partial C_{L_{sty}}}{\partial z} + K_L a_{mix}\left(\frac{C_{G_{sty}}}{H_{mix}} - C_{L_{sty}}\right) - \frac{D_{mix}a}{\beta}(C_{L_{sty}} - S_{sty,1}) \qquad (2)$$

154   Mass balance on the biofilm

155
$$\frac{\partial S_{sty}}{\partial t} = f(X_v)D_{mix}\frac{\partial^2 S_{sty}}{\partial x^2} - \frac{\mu_{max}X_v}{Y_{sty}}\frac{S_{sty}}{S_{sty} + K_{sty}}\frac{S_O}{S_O + K_O} \qquad (3)$$

156

157   2.3. Model calibration and validation

158   Model calibration was performed by fitting the experimental data and model results

159   corresponding to the steady state of the TPPB-BTF performance. The calibration parameters

160   selected were related to the physical properties of styrene: the partition coefficient between

161   gas and the liquid water–silicone mixture (H_{mix}), diffusivity (D_{mix}), and the gas–liquid mass

7

162 transfer coefficient (K_La_{mix}). The remaining parameters were kept the same as those in the

163 styrene-degrading BTF without a NAP ($\delta = 60 \times 10^{-6}$ m, $\beta = 3.8 \times 10^{-6}$ m, $X_v = 50$ kg m^{-3},

164 f(X_v)=0.35, θ_L=0.093, θ_B =0.18, Part1).

165 The mathematical procedure for calibration was similar to that described in Part 1, consisting

166 of the minimization of an objective function defined as the sum of the norm between the

167 experimental and the modeled RE using the algorithm *fminsearch* from MATLAB®. A

168 sensitivity analysis of the calibration parameters was conducted to evaluate their influence on

169 the model predictions. The validation of the model was conducted using the data on the

170 continuous monitoring of the TPPB-BTF under variable styrene inlet loadings, which are

171 operating conditions commonly found in industrial emissions.

172

173 **3. Results and discussion**

174 3.1. Model calibration

175 Model calibration was performed using the data from a TPPB treating styrene at several ILs

176 and EBRTs (San-Valero et al., 2017). The experimental conditions and elimination capacities

177 used for calibration are summarized in Table 1. The results corresponded to the average data

178 from the steady state elimination capacities (ECs) achieved at the end of each experimental

179 period. The calibration procedure resulted in the following apparent parameters: K_La_{mix} of 9.2

180 $\times 10^{-3}$ s^{-1}, D_{mix} of 2.26×10^{-9} m^2 s^{-1}, and H_{mix} of 0.05. These values were obtained by fitting

181 the experimental data to the model prediction, minimizing the sum of the norm between the

182 differences of experimental RE and modeled RE.

183 The mass transfer coefficient obtained here was 19% lower than that in the conventional BTF

184 (K_La of styrene in water of 1.14×10^{-2} s^{-1}, Part 1), thus indicating that the addition of silicone

185 oil increased the mass transfer resistance. Dumont et al. (2014) observed that the silicone oil

186 addition slightly hindered the mass transfer rate compared with the air/water system but that

187   this drop would only be apparent, balancing the greater driving force related to the decrease

188   in the partitioning coefficient. Other authors have suggested that the negative effect of a NAP

189   on the mass transfer coefficient could be explained by the viscosity of the NAP or the

190   formation of a rigid film that causes an increase in the mass transfer resistance (Rols and

191   Goma, 1989; Yeom et al., 2010). Several recent studies have revealed that the effect of the

192   NAP on mass transfer coefficients remained unclear regardless of which solute was used or

193   configuration was applied and that no general trends had been established to date (Dumont

194   and Andrès, 2012; Hernández et al., 2011; Quijano et al., 2009a). The direct comparison of

195   the variation in the K_La of styrene in water–silicone mixtures versus water is not possible for

196   TPPB-BTF due to the lack of literature data. Using a stirred reactor aerated with air polluted

197   with styrene, Dumont and Andrès (2012) obtained a decrease in the ratio of K_La_{mix}/K_La_{water} of

198   0.37, 0.07, and 0.03 for mixtures of silicone oil of 2%, 10%, and 20%, respectively. These

199   authors concluded that to consider K_La a good parameter to characterize the effect of the

200   silicone oil addition in the mass transfer, the partition coefficient value must be consistently

201   expressed in the mass transfer model (H_{water}, H_{NAP}, H_{mix}).

202 The affinity of styrene for silicone oil has been further established in the literature with a

203   well-accepted value of Henry's law constant of styrene in silicone oil (H_{NAP}) of is $4.1 \pm 0.6 \times$

204   10^{-4}, which is approximately 236 times lower than that in water (0.1, Patel et al., 2017). The

205   value of the water–silicone mixture is usually calculated on the basis of the contribution of

206   the percentage of silicone oil and water (Dumont et al., 2010; Hernández et al., 2011; Quijano

207   et al., 2010). In the current study, another approach was used for the first time in which H_{mix}

208   was selected as the calibration parameter for a TPPB-BTF with biomass. It yielded a value of

209   0.05, which was one order of magnitude higher than that predicted by the contribution of the

210   percentage of silicone oil and water according to Henry's law constant of styrene in silicone

211   oil and that in water. The lower increase in the styrene solubility could be attributed to the

212   dynamic associated to the biofilm evolution and to the production of metabolites (i.e., extra-

213   cellular polymeric substances and soluble particulate matter), which could mask, to some

214   extent, the contribution of silicone oil by phenomena such as absorption and/or adsorption.

215   Regarding the third calibration parameter, the value of diffusivity obtained from the water–

216   silicone liquid, D_{mix}, was 2.5 times higher than that in water. Data are lacking related to VOC

217   diffusivity in silicone oil; Dumont et al. (2012) pointed out that the diffusion coefficient of

218   styrene in a silicone oil of five times greater viscosity than water should be around four times

219   higher than that in water according to the general mass transfer enhancement factor model of

220   Zhang et al. (2006), but this was not confirmed experimentally. These authors found that the

221   mass transfer rate in water–silicone oil systems was twice as high as those determined in air–

222   water systems, regardless of the silicone oil volume fraction: 2%, 10%, or 20% or the inlet

223   gas concentration of styrene: 344–1708 mg m^{-3}. In our study, with a silicone oil of higher

224   viscosity (50.0 mPa s^{-1}), the proposed value of the diffusivity for the water–silicone emulsion

225   seems to be in line with this prediction. In the present study, the joint calibration of the three

226   parameters that influenced the mass transfer phenomena confirmed the capacity of the tested

227   water–silicone oil mixture to increase the styrene mass transfer by a factor of 1.6.

228   The high correspondence between the model predictions and the experimental data is shown

229   in Fig. 1, which depicts the relationship between the experimental EC and the modeled EC

230   for the three EBRTs tested. The model simulations predicted all the experimental conditions

231   tested, with a maximum relative error of 11%. Statistical analysis of the normalized mean

232   square error demonstrated a goodness of fit of 0.94. Thus, the model application showed that

233   the change in the physical properties of the liquid film from the styrene-degrading BTF

234   model satisfactorily simulated the steady-state performance of the TPPB-BTF at ILs of 13–77

235   g C m^{-3} h^{-1} and an EBRT of 30–15 s.

236
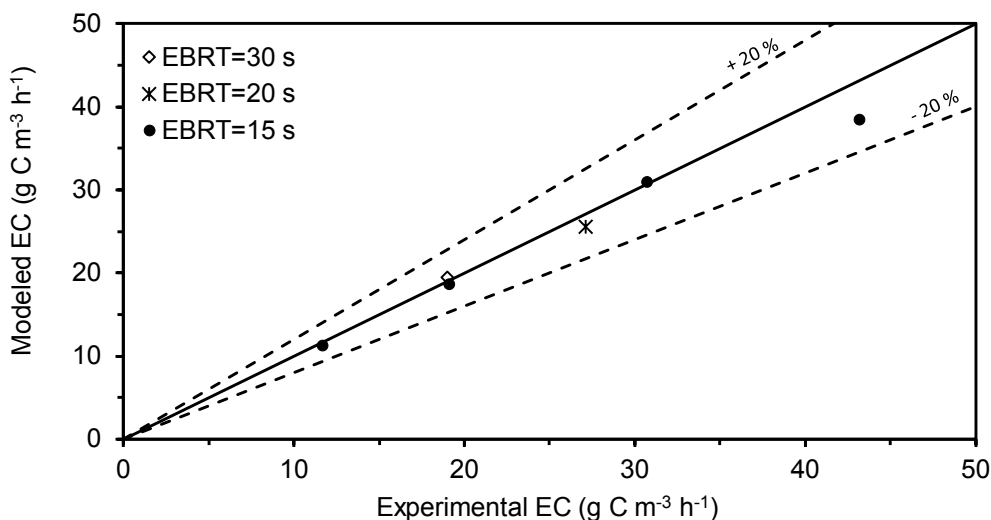
Fig. 1. Comparison between the experimental and the modeled EC of the laboratory TPPB-

BTF from model calibration

To compare the TPPB-BTF and the conventional BTF, the EC curve versus IL at an EBRT of

15 s along with the model simulation for both systems is shown in Fig. 2. As illustrated, the

model predictions reasonably reproduced the ability of the TPPB-BTF to overpass the mass

transfer limitation encountered in a conventional BTF for the removal of styrene. Only slight

discrepancies of the TPPB model were obtained for the highest tested IL: the model EC

prediction was of 38.5 g C m^{-3} h^{-1} versus the experimental value of 43.2 $\pm$ 1.5 g C m^{-3} h^{-1}. By

modifying the selected physical properties of the pollutant, the model successfully predicted

the improvement in the EC due to the increase in the styrene mass transfer by a factor of 1.6

with the NAP addition.
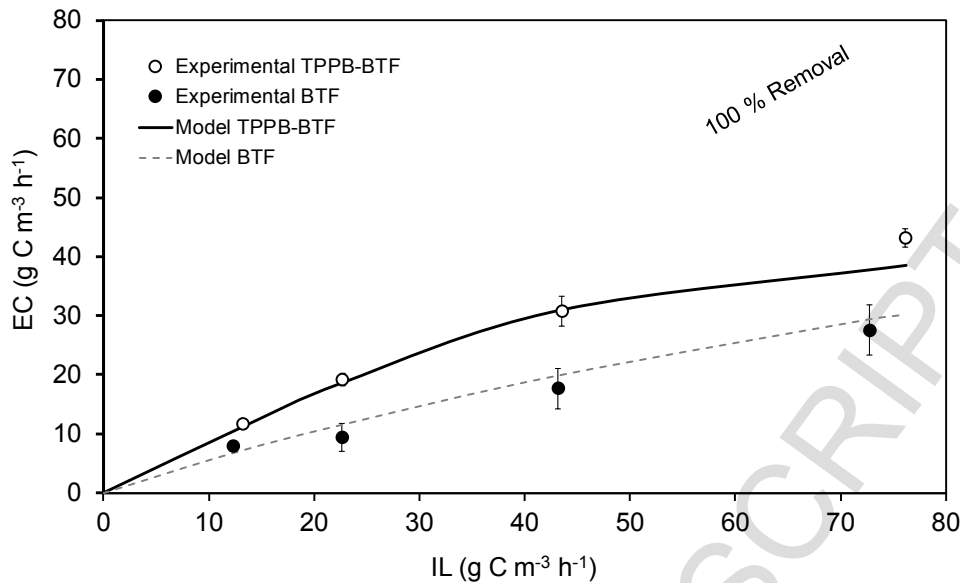
249

250   Fig. 2. Model prediction for the relationship between EC and IL at an EBRT of 15 s: TPPB-

251   BTF vs. BTF and experimental comparison

252

253   3.2 Sensitivity analysis

254   A sensitivity analysis was performed to evaluate the influence of the calibrated parameters on

255   the model predictions. The analysis was performed using the operational conditions

256   corresponding to an IL of 43 g C m^{-3} h^{-1} and an EBRT of 15 s. Model sensitivity was assessed

257   by varying the selected parameters ± 50% and evaluating the effect on the EC, which was

258   selected as the performance variable. The results are shown in Fig. 3. The sensitivity analysis

259   revealed that the calibrated parameters were sensitive at the experimental conditions tested.

260   Moreover, the partition coefficient between gas and the water–silicone mixture was the most

261   sensitive parameter of the model. The mass transfer and the diffusion coefficients had a

262   similar influence on the EC, and their sensitivities increased at the low values of the

263   parameter. For example, a 50% decrease in the $K_L a_{mix}$ and D_{mix} led to a reduction of 13% and

264   8% on the EC, respectively, whereas a 50% increase led to an improvement of 3–4%.
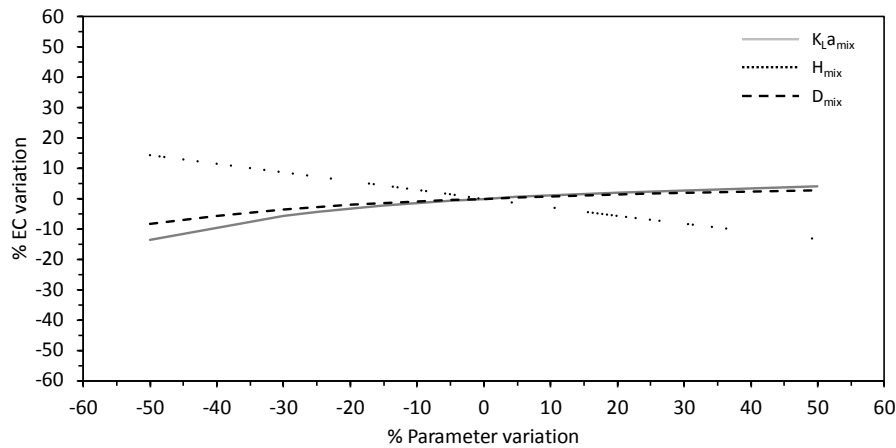
Fig. 3. Sensitivity analysis for the calibrated parameters of the TPPB-BTF model

3.3 Model validation under transient conditions

The model validation was performed by predicting the instantaneous evolution of the outlet

gas phase of styrene in two case studies using the same TPPB-BTF working at an EBRT of

15 s. For this purpose, two different inlet concentration patterns were used. The first pattern

tested involved four cycles of alternating inlet concentrations at ~100–700 mg C m^{-3}, each for

2 h (Fig. 4a). The second pattern tested comprised three cycles of inlet concentration

fluctuations of approximately 100, 250, 400, 550, and 350 mg C m^{-3} (Fig. 4b). The model

predictions, which showed good agreement, are shown in Fig. 4. The slight differences in the

dynamic between the experimental data and the model predictions in the outlet gas phase

concentration could be attributed to dynamic phenomena, such as instantaneous absorption

on the biofilm that is not accounted for in the present model. The model predicted a drastic

drop in the TPPB-BTF performance from an RE of approximately 80% at an inlet

concentration of ~100 mg C m^{-3} to a RE of ~20% at an inlet concentration peak of ~700 mg

C m^{-3} (Fig. 4a). The model consistently predicted the dynamic response in the outlet

concentration when the inlet concentration increased and of the time required to recover the

nominal conditions when the inlet concentration decreased to approximately 100 mg C m^{-3}.

Therefore, the model predictions indicate that under dynamic conditions, the TPPB-BTF

13

285   could recover the previous high RE after applying a peak of concentration nearly seven times

286   higher than the nominal one. Fig. 4b illustrates the dynamic response of the TPPB-BTF and

287   the model simulation when the second styrene feeding was applied. This figure shows the

288   capability of the model to simulate the variation of the outlet concentration with the RE at

289   80% and 55%, for inlet concentrations of ~100 mg C m^{-3} and ~350 mg C m^{-3}, respectively.

290   At high inlet concentrations (~450 and 550 mg C m^{-3}) the REs dropped up to 40%. This

291   result indicates that the model developed here can be used as a powerful tool for predicting

292   the TPPB-BTF performance under steady and transient conditions. In addition, the response

293   of the treatment system toward unexpected styrene shock loadings can be anticipated through

294   model simulations, allowing the development of operating protocols for pollutant shock

295   loading.
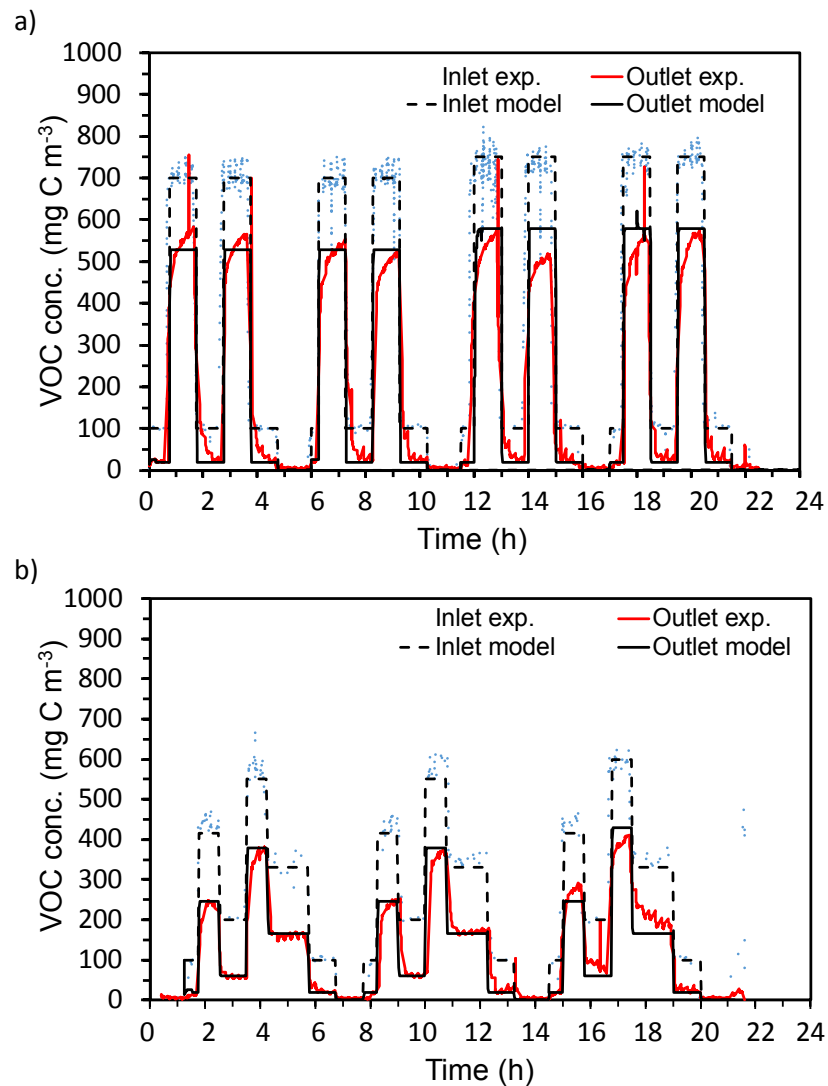
Fig. 4. Experimental data and model predictions of the TPPB-BTF from variations in the inlet
styrene concentration in the lab-scale TPPB-BTF (EBRT of 15 s).

3.4 Comparison between TPPB-BTF and conventional BTF

The developed models for conventional BTF (Part 1) and TPPB-BTF (Part 2) were used to

compare their performance under different operational conditions to demonstrate the

applicability and usefulness of the modeling approach and the potential performance

improvement caused by adding silicone oil. First, the model from Part 1 was used to predict

the response of a styrene-degrading BTF from the literature (Pérez et al., 2015) to show its

applicability in a wide range of operational conditions. Then, the TPPB-BTF model was used

307   to estimate the improvement in terms of EC that would have been achieved if silicone oil had

308   been added.

309   The first scenario corresponds to a BTF treating styrene with an IL of 12–38 g m^{-3} h^{-1}, an

310   EBRT of 30–60 s and an intermittent irrigation (15 min every 2 h) from Pérez et al. (2015).

311   The compilation of the experimental data is shown in Table 2. The results from the model

312   simulation along with the experimental data are depicted in Fig. 5. The high grade of

313   correspondence (goodness of fit of 0.91) corroborates that the model developed for a styrene-

314   degrading BTF is valid in the typical range of design and operational parameters. The BTF

315   treating styrene fully degraded styrene (RE > 90%) at a maximum IL of 15 g C m^{-3} h^{-1}

316   (EBRT = 60 s). Further increases in the IL by decreasing the EBRT or by increasing the inlet

317   concentration hindered the RE up until 75%. The model predicted this behavior at an EBRT

318   of 45–60 s, which was unlike that used for calibration (15–30 s). Thus, the model's suitability

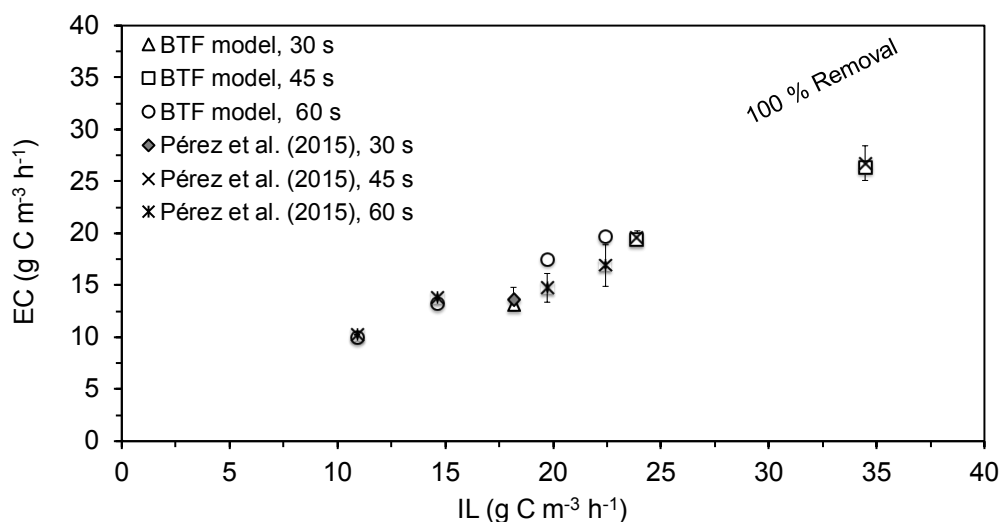319   was successfully validated in the wide range of EBRTs of 15–60 s and ILs of 10–77 g C m^{-3}

320   h^{-1}.

321

322   Table 2. Compilation of experimental styrene removal performance from Pérez et al. (2015)

C_{in} (mg Nm^{-3})	EBRT (s)	C_{out} (mg Nm^{-3})	RE (%)	IL (g m^{-3} h^{-1})	EC (g m^{-3} h^{-1})
216 ± 14	60	13	94	12	11
290 ± 12	60	29	90	16	14
391 ± 3	60	99 ± 28	75	22	16
444 ± 39	60	109 ± 40	75	24	18
355 ± 50	45	64 ± 10	82	26	21
512 ± 5	45	115 ± 25	78	38	29
180 ± 0	30	45 ± 11	75	20	15

323
324

325

326   Fig. 5. Application of the BTF model to simulate the literature data on styrene-degrading

327   BTF (Pérez et al., 2015)

328

329   The TPPB-BTF model was applied to evaluate the potential improvements in the styrene

330   removal of this BTF. Fig. 6 summarizes the comparison between both models (BTF-Part 1

331   and the TPPB-BTF). This BTF system was mass transfer limited for the tested ILs and

332   EBRTs. For all data, the TPPB-BTF model predicted an improvement in the EC, which was

333   related to the enhancement of the styrene mass transfer in the water–silicone/air system in

334   comparison with the water/air system. This improvement increased the critical IL; this effect

335   was more noticeable for shorter EBRTs (45 and 30 s). These results strongly suggested that

336   using TPPB-BTF for styrene abatement could be recommended in mass transfer limited

337   systems. The model approach is shown as a valuable tool in the design and operation of

338   TPPB-BTFs.

339   This is the first attempt to model a TPPB-BTF with biomass operated under typical

340   conditions found in industrial BTFs. Further investigation on the influence of the percentage

341   of silicone oil in the sensitivity of the model parameters would expand its applicability.

342

17
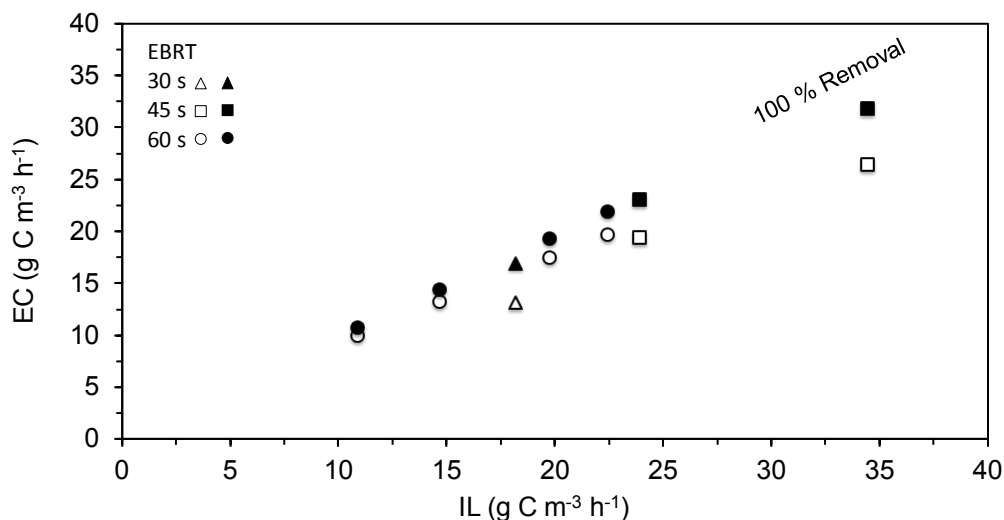
Fig. 6. Potential improvement in styrene removal by adding silicone oil according to model predictions. Open symbols correspond to BTF and solid symbols to the TPPB-BTF.

4. Conclusions

A dynamic model to simulate TPPB-BTFs was developed, calibrated, and validated by extending the modeling approach used in Part 1 for conventional BTFs. The styrene removal of a laboratory TPPB-BTF was successfully simulated by modifying the physical properties of styrene in the water–silicone liquid mixture, accurately predicting the enhanced outlet performance. Moreover, the model predicted, with a high grade of correspondence, the transient conditions by simulating the peaks of the emissions associated with the high fluctuations in the inlet concentration. Model predictions consistently proved that the presence of silicone oil improved the removal of styrene by BTFs by enhancing diffusion and solubility, although mass transfer resistance increased by 19%. To the best of our knowledge, this work is the first on the mathematical modeling of TPPB-BTFs operated under dynamic conditions according to industrial applications.

366 **References**

367 Bailón, L., Nikolausz, M., Kästner, M., Veiga, M.C., Kennes, C., 2009. Removal of

368   dichloromethane from waste gases in one- and two-liquid-phase stirred tank bioreactors

369   and biotrickling filters. Water Res. 43, 11–20. doi:10.1016/j.watres.2008.09.031

370 Darracq, G., Couvert, A., Couriol, C., Amrane, A., Le Cloirec, P., 2012. Removal of

371   hydrophobic volatile organic compounds in an integrated process coupling absorption

372   and biodegradation-selection of an organic liquid phase. Water. Air. Soil Pollut. 223,

373   4969–4997. doi:10.1007/s11270-012-1251-0

374 Daugulis, A.J., Tomei, M.C., Guieysse, B., 2011. Overcoming substrate inhibition during

375   biological treatment of monoaromatics: recent advances in bioprocess design. Appl.

376   Microbiol. Biotechnol. 90, 1589–608. doi:10.1007/s00253-011-3229-z

377 Dorado, A.D., Dumont, E., Muñoz, R., Quijano, G., 2015. A novel mathematical approach

378   for the understanding and optimization of two-phase partitioning bioreactors devoted to

379   air pollution control. Chem. Eng. J. 263, 239–248. doi:10.1016/j.cej.2014.11.014

380 Dumont, E., Andrès, Y., 2012. Styrene absorption in water/silicone oil mixtures. Chem. Eng.

381   J. 200–202, 81–90. doi:10.1016/j.cej.2012.06.028

382 Dumont, E., Andrès, Y., Le Cloirec, P., 2014. Mass transfer coefficients of styrene into

383   water/silicone oil mixtures: New interpretation using the "equivalent absorption

384   capacity" concept. Chem. Eng. J. 237, 236–241. doi:10.1016/j.cej.2013.10.021

385 Dumont, E., Darracq, G., Couvert, A., Couriol, C., Amrane, A., Thomas, D., Andrès, Y., Le

386 Cloirec, P., 2010. Determination of partition coefficients of three volatile organic

387 compounds (dimethylsulphide, dimethyldisulphide and toluene) in water/silicone oil

388 mixtures. Chem. Eng. J. 162, 927–934. doi:10.1016/j.cej.2010.06.045

389 Hernández, M., Quijano, G., Muñoz, R., Bordel, S., 2011. Modeling of VOC mass transfer in

390 two-liquid phase stirred tank, biotrickling filter and airlift reactors. Chem. Eng. J. 172,

391 961–969. doi:10.1016/j.cej.2011.07.008

392 Karimi, A., Golbabaei, F., Neghab, M., Pourmand, M.R., Nikpey, A., Mohammad, K.,

393 Mehrnia, M.R., 2013. Biodegradation of high concentrations of benzene vapors in a two

394 phase partition stirred tank bioreactor. Iranian J. Environ. Health Sci. Eng. 10, 10.

395 doi:10.1186/1735-2746-10-10

396 Kraakman, N.J.R., Rocha-Rios, J., van Loosdrecht, M.C.M., 2011. Review of mass transfer

397 aspects for biological gas treatment. Appl. Microbiol. Biotechnol. 91, 873–886.

398 doi:10.1007/s00253-011-3365-5

399 Moradkhani, H., Izadkhah, M.S., Anarjan, N., 2017. Experimental and CFD-PBM study of

400 oxygen mass transfer coefficient in different impeller configurations and operational

401 conditions of a two-phase partitioning bioreactor. Appl. Biochem. Biotechnol. 181, 710–

402 724. doi:10.1007/s12010-016-2243-0

403 Muñoz, R., Chambaud, M., Bordel, S., Villaverde, S., 2008. A systematic selection of the

404 non-aqueous phase in a bacterial two liquid phase bioreactor treating α-pinene. Appl.

405 Microbiol. Biotechnol. 79. doi:10.1007/s00253-008-1400-y

406 Muñoz, R., Daugulis, A.J., Hernández, M., Quijano, G., 2012. Recent advances in two-phase

407 partitioning bioreactors for the treatment of volatile organic compounds. Biotechnol.

408 Adv. 30, 1707–20. doi:10.1016/j.biotechadv.2012.08.009

409 Ordaz, A., López, J.C., Figueroa-González, I., Muñoz, R., Quijano, G., 2014. Assessment of

410 methane biodegradation kinetics in two-phase partitioning bioreactors by pulse

411   respirometry. Water Res. 67C, 46–54. doi:10.1016/j.watres.2014.08.054

412   Parnian, P., Zamir, S.M., Shojaosadati, S.A., 2016. Styrene vapor mass transfer in a

413   biotrickling filter: Effects of silicone oil volume fraction, gas-to-liquid flow ratio, and

414   operating temperature. Chem. Eng. J. 284, 926–933. doi:10.1016/j.cej.2015.08.148

415   Patel, M.J., Popat, S.C., Deshusses, M.A., 2017. Determination and correlation of the

416   partition coefficients of 48 volatile organic and environmentally relevant compounds

417   between air and silicone oil. Chem. Eng. J. 310, 72–78. doi:10.1016/j.cej.2016.10.086

418   Pérez, M.C., Álvarez-Hornos, F.J., Portune, K., Gabaldón, C., 2015. Abatement of styrene

419   waste gas emission by biofilter and biotrickling filter: comparison of packing materials

420   and inoculation procedures. Appl. Microbiol. Biotechnol. 99, 19–32.

421   doi:10.1007/s00253-014-5773-9

422   Quijano, G., Chávez-Avila, R., Muñoz, R., Thalasso, F., Ordaz, A., 2010. KLa measurement

423   in two-phase partitioning bioreactors: New insights on potential errors at low power

424   input. J. Chem. Technol. Biotechnol. 85, 1407–1412. doi:10.1002/jctb.2460

425   Quijano, G., Hernandez, M., Thalasso, F., Muñoz, R., Villaverde, S., 2009a. Two-phase

426   partitioning bioreactors in environmental biotechnology. Appl. Microbiol. Biotechnol.

427   84, 829–846. doi:10.1007/s00253-009-2158-6

428   Quijano, G., Revah, S., Gutiérrez-Rojas, M., Flores-Cotera, L.B., Thalasso, F., 2009b.

429   Oxygen transfer in three-phase airlift and stirred tank reactors using silicone oil as

430   transfer vector. Process Biochem. 44, 619–624. doi:10.1016/j.procbio.2009.01.015

431   Rene, E.R., Montes, M., Veiga, M.C., Kennes, C., 2011. Styrene removal from polluted air in

432   one and two-liquid phase biotrickling filter: steady and transient-state performance and

433   pressure drop control. Bioresour. Technol. 102, 6791–800.

434   doi:10.1016/j.biortech.2011.04.010

435   Rols, J.L., Goma, G., 1989. Enhancement of oxygen transfer rates in fermentation using

436   oxygen-vectors. Biotechnol. Adv. 7, 1–14. doi:10.1016/0734-9750(89)90900-2

437   San-Valero, P., Gabaldón, C., Penya-roja, J.M., Quijano, G., 2017. Enhanced styrene removal

438   in a two-phase partitioning bioreactor operated as a biotrickling filter: Towards full-

439   scale applications. Chem. Eng. J. 309, 588–595. doi:10.1016/j.cej.2016.10.054

440   San-Valero, P., Penya-Roja, J.M., Álvarez-Hornos, F.J., Marzal, P., Gabaldón, C., 2015.

441   Dynamic mathematical modelling of the removal of hydrophilic VOCs by biotrickling

442   filters. Int. J. Environ. Res. Public Health 12, 746–766. doi:10.3390/ijerph120100746

443   Sempere, F., Martínez-Soria, V., Penya-Roja, J.M., Waalkens, A., Gabaldón, C., 2012.

444   Control of VOC emissions from a flexographic printing facility using an industrial

445   biotrickling filter. Water Sci. Technol. 65, 177–82. doi:10.2166/wst.2011.839

446   Yeom, S.H., Daugulis, A.J., Nielsen, D.R., 2010. A strategic approach for the design and

447   operation of two-phase partitioning bioscrubbers for the treatment of volatile organic

448   compounds. Biotechnol. Prog. 26, 1777–1786. doi:10.1002/btpr.481

449   Zamir, S.M., Babatabar, S., Shojaosadati, S.A., 2015. Styrene vapor biodegradation in single-

450   and two-liquid phase biotrickling filters using Ralstonia eutropha. Chem. Eng. J. 268,

451   21–27. doi:10.1016/j.cej.2015.01.040

452   Zhang, G.D., Cai, W.F., Xu, C.J., Zhou, M., 2006. A general enhancement factor model of

453   the physical absorption of gases in multiphase systems. Chem. Eng. Sci. 61, 558–568.

454   doi:10.1016/j.ces.2005.07.035

455

456

457 **Nomenclature**

a	Specific surface area of the packing material
C	Concentration
D	Diffusion coefficient
f(Xv)	Correction factor of diffusivity in the biofilm according to Fan's equation
H	Partitioning coefficient
K	Half saturation rate constant of the substrate
$K_L a$	Overall mass transfer coefficient of the substrate
S	Concentration in the biofilm
t	Time
v	Superficial velocity
x	Coordinate for the depth in the biofilm
X_v	Biomass concentration in the biofilm
Y	Yield coefficient
z	Axial coordinate in the reactor from the inlet to the outlet
Greek letters	
β	Thickness of the liquid film
δ	Thickness of the biofilm
$θ_B$	Volume fraction occupied by the biofilm
$θ_G$	Porosity of the bioreactor
$θ_L$	Volume fraction occupied by the liquid film
$θ_P$	Void space of the packing material
$μ_{max}$	Maximum specific growth rate of the substrate
Subscripts	
G	Gas
L	Liquid
B	Biofilm
mix	Properties of styrene in the pseudo-homogeneous water–silicone mixture
Sty	Styrene
O	Oxygen

458

23